

Multimodal Large Language Models with Adaptive Preference Optimization for Sequential Recommendation

Yu Wang

Hefei University of Technology
Hefei, China
wangyu20001162@gmail.com

Yonghui Yang

National University of Singapore
Singapore, Singapore
yyh.hfut@gmail.com

Le Wu

Hefei University of Technology
Hefei, China
lewu.ustc@gmail.com

Yi Zhang

Auhui University
Hefei, China
zhangyi.ahu@gmail.com

Richang Hong

Hefei University of Technology
Hefei, China
hongrc.hfut@gmail.com

Abstract

Recent advances in Large Language Models (LLMs) have opened new avenues for sequential recommendation by enabling natural language reasoning over user behavior sequences. A common approach formulates recommendation as a language modeling task, where interaction histories are transformed into prompts and user preferences are learned via supervised fine-tuning. However, these methods operate solely in the textual modality and often miss users' fine-grained interests, especially when shaped by rich visual signals such as product images or movie posters. Multimodal Large Language Models (MLLMs) offer a promising alternative by aligning text and vision in a shared semantic space. A prevalent training paradigm applies Supervised Fine-Tuning (SFT) followed by Direct Preference Optimization (DPO) to model user preferences. Yet, two core challenges remain: 1) Imbalanced sample hardness, where random negative sampling causes overfitting on easy examples and under-training on hard ones; 2) Cross-modal semantic bias, where the fixed reference model in DPO prevents the policy model from correcting modality misalignments—especially over long sequences. To address these issues, we propose a Multimodal LLM framework that integrates *Hardness-aware and Noise-regularized preference optimization for Recommendation (HaNoRec)*. Specifically, HaNoRec dynamically adjusts optimization weights based on both the estimated hardness of each training sample and the policy model's real-time responsiveness, prioritizing harder examples. It further introduces Gaussian-perturbed distribution optimization on output logits to enhance cross-modal semantic consistency and reduce modality bias inherited from the reference model.

CCS Concepts

- Information systems → Recommender systems.

Keywords

Sequential Recommendation, Multimodal Large Language Models, Preference Alignment

1 Introduction

Recently, Large Language Models (LLMs [11, 44, 64]) have achieved significant progress in tasks such as natural language understanding [10], semantic reasoning [49], and knowledge generalization [7]. This advancement motivates researchers to explore their potential

applications in broader tasks [9, 36, 51]. Especially in Recommender Systems (RS [15, 38, 39]), effectively capturing users' long-term preferences and dynamic needs remains a core challenge. Sequential Recommendation (SR [21, 42, 52]) methods focus on mining users' historical interaction sequences to infer the content they may be interested in next, and LLMs' superior contextual comprehension and generative abilities offer new opportunities in SR. As shown in Figure 1 (a), the left side illustrates the LLM-based SR paradigm, where many studies [5, 6, 57] convert behavioral sequences into textual input prompts. For example, the user has watched the following movies: $[item_1], [item_2], \dots, [item_n]$. Please write a movie that the user may watch: $[candidate_1], [item_{n+1}], \dots, [candidate_k]$. However, LLMs typically focus solely on textual information and struggle to fully exploit the multimodal data [56] (e.g., images and video) that are prevalent in recommendation tasks, limiting their ability to understand rich and diverse recommendation contexts.

Some studies [61, 63, 66] explore applying soft prompt strategies to multimodal information to alleviate the above limitations. For example, in Figure 1 (a), they use a frozen visual encoder to extract image features and project them into the LLM-based SR framework as tokens to improve recommendation performance. Although this strategy partially utilizes image information and yields performance improvements, the LLM itself lacks multimodal alignment training [24], limiting its understanding of image semantics and deep connections between visual and textual data. In contrast, Multimodal Large Language Models (MLLMs [3, 23, 33]) successfully align multimodal information into a unified semantic space through joint pre-training tasks [3], shared encoder architectures [23], cross-modal contrast [33], and large-scale data training [1]. This capability not only enhances the model's understanding of multimodal data but also offers new possibilities for multimodal modeling in recommender systems. As shown in the bar chart in Figure 1 (a), MLLMs demonstrate higher hit ratios across all datasets, significantly outperforming LLMs and soft prompt methods, proving the advantages of MLLMs in multimodal recommendation. Nevertheless, enabling MLLMs to effectively capture the evolution of user preferences in SR remains some significant challenges, as follow:

- **Imbalanced Sample Hardness.** Existing MLLM-based SR methods [54, 67] generally adopt Supervised Fine-Tuning (SFT [6, 54]), which focuses on observed historical behaviors while overlooking fine-grained changes in user preferences. Direct Preference Optimization (DPO [12, 25]) further addresses this limitation by

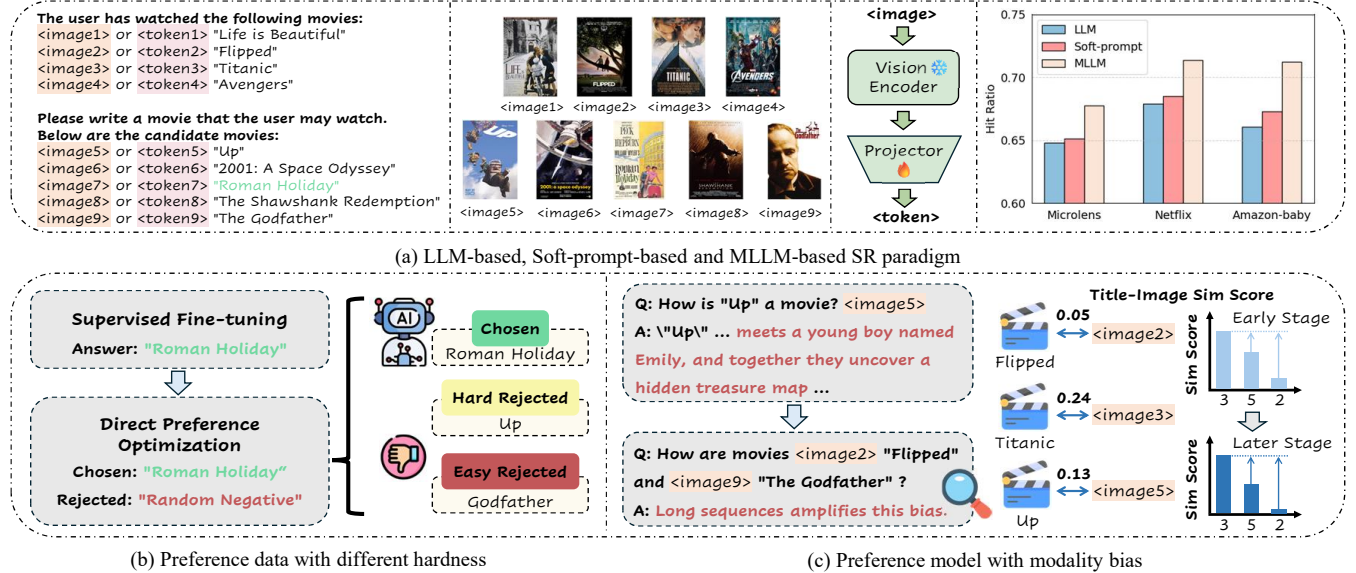


Figure 1: (a) Existing paradigms and performance comparisons of large model-based sequential recommendation; (b) Data construction and sample hardness issues in MLLM-SR during DPO training; (c) Title-image similarity scores exhibit a “the weak get weaker” trend due to MLLM modality bias after DPO training.

leveraging the differences between preference data. As shown in Figure 1 (b), SFT-based models construct DPO data by randomly sampling rejected examples from user interactions. However, this strategy results in noticeable imbalance across sample hardness levels, with the model favoring repeated training on easy contrasts and struggling to distinguish borderline cases or nuanced preferences. For example, an easy-to-distinguish sample like the “*Godfather*” shows a large semantic gap with the positive sample “*Roman Holiday*”, while the gap is much smaller with “*Up*”, a semantically short and modality bias-prone sample. During DPO training, the reward gap continually amplifies the optimization of easy-to-distinguish samples while neglecting hard-to-distinguish ones, thus failing to fully capture hidden sequential preference signals. Therefore, designing a reweighting strategy that perceives variations in sample hardness is crucial.

- **Cross-modal Semantic Bias.** Nevertheless, a significant barrier in our alignment process is modality bias [43, 45, 65], which occurs when the MLLM-based SR model fails to accurately interpret semantic information from an item’s title and image, particularly in cases with ambiguous or short movie titles. As shown in Figure 1 (c), the model misdescribes “*Up*” (a film about adventure in a flying house) as “searching for hidden treasure”. Furthermore, user histories often contain multiple such potentially ambiguous or thematically similar movies, and SR-based long sequences tend to amplify modality bias by accumulating these local semantic drifts [47, 54]. Accordingly, we calculate the title-image similarity scores throughout the alignment process, as illustrated in part (c). It can be observed that, samples with initially high similarity (e.g., “*Titanic*”) remain stable or even slightly improve in the later stage. In contrast, samples with low initial similarity (such as “*Flipped*”) show further score decline, indicating a “the weak get weaker” trend in representation degradation. Therefore,

a sequence and distribution-sensitive optimization strategy for title-image similarity is needed.

To tackle the challenges mentioned above, we propose a preference optimization framework, named ***Hardness-aware and Noise-regularized preference optimization for Recommendation (HaNoRec)***. For **Challenge 1**, we design a **Hardness-aware Reweighting Strategy (HaRS)**, where the dynamic scaling factor β is proportional to sample hardness to mitigate sample imbalance and focus optimization on challenging cases. **In a nutshell, a larger factor constrains model updates, while a smaller factor encourages optimization [34].** Specifically, HaRS employs a specific MLLM encoder to convert multimodal information into semantic representations, calculates similarity scores to form positive-negative sample pairs for hardness estimation. It also evaluates model responsiveness through the normalized reward gap of each sample pair, and removes outliers. For **Challenge 2**, we devise a **Noise-regularized Distribution Optimization (NoDO)** objective to mitigate cross-modal bias from ambiguous titles and maintain representational consistency in long sequences. NoDO introduces Gaussian noise perturbations to smoothly model the representation distributions of the current model and the reference model. It estimates their distributional distance in the title-image semantic space, and adaptively adjusts alignment constraints via KL divergence [2]. The contributions are summarized as follows:

- We investigate the application of MLLMs to sequential recommendation (SR) and design a hardness-aware reweighting strategy that effectively addresses sample imbalance and enhances the model’s sensitivity to subtle shifts in user preferences.
- We further devise a noise-regularized distribution optimization objective, which aligns cross-modal title–image pairs via Gaussian noise perturbation and KL divergence-based constraints, thereby mitigating modality bias arising from weak semantics.

- Extensive experiments on three benchmark datasets demonstrate that our approach consistently outperforms existing baselines. Furthermore, we provide a thorough analysis of the contributions of both the reweighting strategy and the distribution optimization method to SR performance.

2 Preliminary

In this section, we first introduce the problem of general sequential recommendation, the present how we integrate MLLMs to empower sequential recommendation through SFT and DPO manners.

Problem Formulation. In a general sequential recommendation scenario, we consider a user set \mathcal{U} and an item set \mathcal{V} , where $|\mathcal{U}|$ and $|\mathcal{V}|$ denote the total number of users and items, respectively. The goal is to model dynamic user interests over time by leveraging their historical interaction behaviors. Formally, given an interaction sequence $S^u = \{v_1^u, v_2^u, \dots, v_t^u\}$ for a user $u \in \mathcal{U}$, where v_t^u is the item interacted with at timestamp t , and t indicates the sequence length, the objective is to learn a recommendation function f_θ that predicts the next item v_{t+1}^u the user is most likely to engage with.

Supervised Fine-Tuning (SFT). The process of learning user preferences using an MLLM π typically starts with an SFT phase, yielding a model denoted as π_{SFT} . Specifically, this stage involves adapting the pre-trained MLLM to multimodal tasks by fine-tuning it on a large-scale dataset $\mathcal{D} = \{x, \mathcal{I}, y\}$ composed of question–answer pairs, where x is an instruction, \mathcal{I} is the corresponding image input, and y is the expected response generated by the model. Following the setting in [54], each training sample (x, \mathcal{I}, y) is built from the user's interaction history. The instruction x encodes the interaction sequence S^u and a candidate set containing the ground-truth next item v_{t+1}^u . The image input \mathcal{I} includes visuals of items in S^u and v_{t+1}^u . The expected response y is the ground-truth item v_{t+1}^u , which the model learns to generate or identify. The SFT objective aims to maximize the likelihood of generating the expected response y conditioned on the instruction x and the visual input \mathcal{I} . Formally, the training objective is:

$$\mathcal{L}_{\text{SFT}} = -\mathbb{E}_{(x, \mathcal{I}, y) \sim \mathcal{D}} [\log \pi_{\text{SFT}}(y | \mathcal{I}, x)]. \quad (1)$$

Direct Preference Optimization (DPO). Following Supervised Fine-Tuning (SFT), preference learning in MLLM-based recommendation is typically approached via *Reinforcement Learning from Human Feedback (RLHF)*. In this setting, preference data are constructed as response pairs (y_w, y_l) , where y_w denotes the ground-truth next item and y_l is a randomly sampled unobserved item. Classical RLHF involves two stages: (1) training a reward model $r_\phi(y | \mathcal{I}, x)$ to reflect user preference by scoring y_w higher than y_l ; and (2) optimizing the policy model π_θ via reinforcement learning, such as Proximal Policy Optimization (PPO [40]), to align with the reward signal while remaining close to a reference model π_{ref} :

$$\begin{aligned} \max_{\pi_\theta} & \mathbb{E}_{(\mathcal{I}, x) \sim \mathcal{D}, y \sim \pi_\theta(\cdot | \mathcal{I}, x)} \left[r_\phi^*(y | \mathcal{I}, x) \right] \\ & -\beta \cdot D_{\text{KL}} [\pi_\theta(y | \mathcal{I}, x) \| \pi_{\text{ref}}(y | \mathcal{I}, x)]. \end{aligned} \quad (2)$$

To reduce the computational overhead of reward model training, *Direct Preference Optimization (DPO)* [34] has been proposed as a more efficient alternative. Instead of learning an explicit reward function, DPO directly optimizes the target policy π_θ using pairwise preference data, relying on implicit feedback embedded in the

preference pairs. Its objective compares the log-likelihood ratios between preferred and rejected responses under both the policy and reference models:

$$\begin{aligned} \mathcal{L}_{\text{DPO}} = & -\mathbb{E}_{(\mathcal{I}, x, y_w, y_l)} [\log \sigma \left(\beta \log \frac{\pi_\theta(y_w | \mathcal{I}, x)}{\pi_{\text{ref}}(y_w | \mathcal{I}, x)} \right) \\ & - \beta \log \frac{\pi_\theta(y_l | \mathcal{I}, x)}{\pi_{\text{ref}}(y_l | \mathcal{I}, x)} \big)]. \end{aligned} \quad (3)$$

Here, β is a hyperparameter controlling the trade-off between divergence regularization and preference alignment. **A larger β emphasizes staying close to the reference model by minimizing KL divergence, while a smaller β encourages stronger preference-driven updates** [34, 45]. While effective, the standard DPO framework still overlooks key factors in multimodal recommendation, sample hardness, and cross-modal semantic misalignment. Next, we present our solution in detail.

3 Methodology

Here, we introduce the technical implementation of our proposed *Hardness-aware and Noise-regularized preference optimization for Recommendation (HaNoRec)*. As shown in Figure 2, HaNoRec consists of two elaborated modules: Hardness-aware Reweighting Strategy (HaRS) and Noise-regularized Distribution Optimization (NrDO). Among them, HaRS dynamically adjusts the optimization emphasis for each training sample based on its hardness and the policy model's responsiveness, ensuring that the model allocates more learning capacity to informative, hard-to-distinguish examples. NrDO, on the other hand, aims to alleviate modality bias by enhancing cross-modal semantic alignment.

3.1 Hardness-aware Reweighting Strategy

While DPO leverages preference pairs to optimize ranking performance, it relies on a fixed weighting scheme that may inadvertently reinforce easy samples while neglecting harder, more informative ones. To address this, we propose an adaptive weighting mechanism for the DPO scaling factor β (refer to Eq. (3)) that dynamically modulates the learning signal based on sample hardness and model responsiveness. Formally, the training data are defined as $\mathcal{D} = \{(\mathcal{I}, x, y_w, y_l)\}$, where \mathcal{I} denotes the image input, x the instruction or query, and y_w, y_l are the preferred and less preferred responses, respectively. Prior to training, we employ a pretrained MLLM [3] to encode the item title set \mathcal{V} and its corresponding image set \mathcal{I} into semantic representations: a textual embedding matrix $\mathbf{H} \in \mathbb{R}^{|\mathcal{V}| \times d}$ and a visual embedding matrix $\mathbf{X} \in \mathbb{R}^{|\mathcal{I}| \times d}$, where d is the shared embedding dimension. To estimate sample hardness, we use the chosen (y_w) and rejected (y_l) items as anchors to compute their semantic similarity with all candidates in the embedding space. Specifically, we calculate similarity scores and retrieve the Top-K most similar items for each anchor, forming positive and negative sample clusters. These clusters serve as a proxy to quantify the contextual indistinguishability of each training pair—samples with overlapping clusters are considered harder and are thus assigned greater weight during optimization.

$$\mathcal{S}_* = \text{Top-K}_{v_j \in \mathcal{V}} \left(\frac{(\mathbf{h}_j + \mathbf{x}_j)^\top (\mathbf{h}_{y_*} + \mathbf{x}_{y_*})}{\|\mathbf{h}_j + \mathbf{x}_j\|_2 \|\mathbf{h}_{y_*} + \mathbf{x}_{y_*}\|_2} \right), \quad * \in \{w, l\} \quad (4)$$

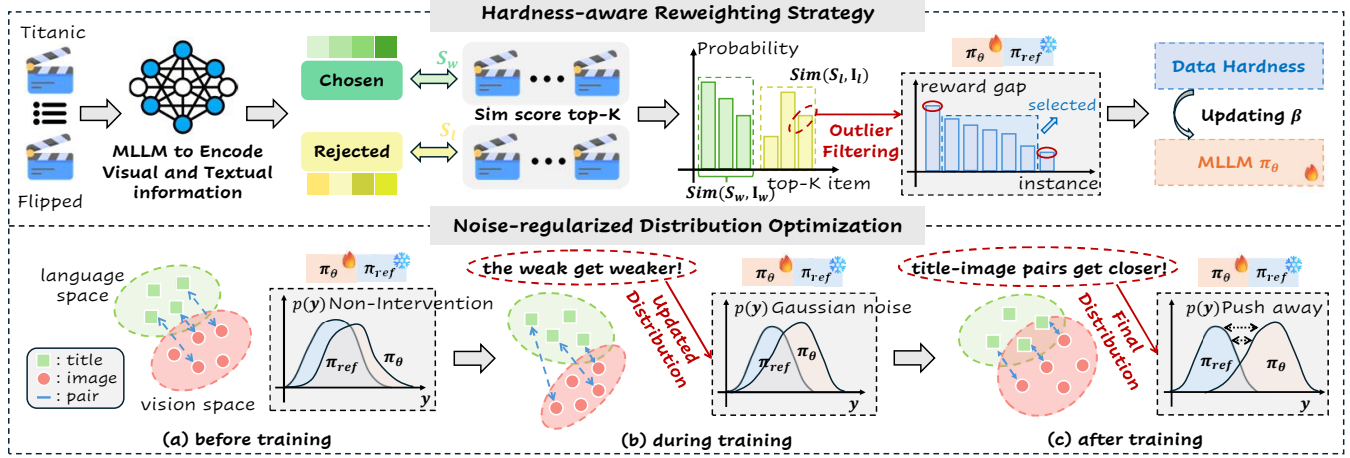


Figure 2: Illustration of HaNoRec. Hardness-aware Reweighting Strategy (HaRS) scales DPO weight proportionally to sample hardness, spotlighting challenging cases. Noise-regularized Distribution Optimization (NoDO) adds Gaussian noise and adaptive KL to align title–image semantics and curb modality bias.

where $(\mathbf{h}_j + \mathbf{x}_j)$ denotes the embedding of item v_j , and $(\mathbf{h}_{y_*} + \mathbf{x}_{y_*})$ represents the embedding of the corresponding target item. This sampling strategy captures multi-granularity preference signals, where varied positive samples reflect different aspects of preference (e.g., genre, style, visuals), and diverse negative samples provide gradients from easy to hard, enabling fine-grained ranking [25]. After obtaining sample sets $\mathcal{S}_w = \{\mathcal{S}_{w,1}, \mathcal{S}_{w,2}, \dots, \mathcal{S}_{w,K}\}$ and $\mathcal{S}_l = \{\mathcal{S}_{l,1}, \mathcal{S}_{l,2}, \dots, \mathcal{S}_{l,K}\}$, where K denotes the number of Top-K similar items. Finally, we calculate $\text{sim}(\mathcal{S}_w, \mathcal{I}_w)$ and $\text{sim}(\mathcal{S}_l, \mathcal{I}_l)$ to estimate sample hardness and determine the dynamic β .

$$\mathbf{Z}_* = \text{Softmax}(\left[\text{sim}(\mathcal{I}_*, \mathcal{S}_{*,k}) \right]_{k=1}^K), * \in \{w, l\}. \quad (5)$$

where $\text{sim}(\cdot)$ denotes the cosine similarity function, and \mathbf{Z}_w and \mathbf{Z}_l represent the probabilities of preferred and rejected samples, respectively. In this step, we average the scores in \mathcal{S}_w to normalize sets of different sizes or ranges before applying Softmax function, avoiding dominance by set size or outliers and ensuring stable, differentiable probability distributions. The difference between the preferred and rejected probabilities indicates the data hardness, which can be defined as:

$$\Delta = \|\mathbf{Z}_{w,k} - \mathbf{Z}_{l,k}\|_{k=1}^K, \quad \lambda = \sigma(\Delta)/\sigma(\bar{\Delta}) \quad (6)$$

where Δ denotes the difference. The final data hardness λ is computed by projecting Δ into the $(0, 1)$ range using the sigmoid function $\sigma(\cdot)$, where $\bar{\Delta}$ is the average difference over the dataset. A larger hardness indicates an “easy-to-distinguish” instance, where the preferred sample aligns clearly with image–text semantics, increasing model confidence. A smaller hardness implies a “hard-to-distinguish” instance, where positive and negative samples are semantically or visually similar, making differentiation difficult and requiring a lower weight β and more optimization attention.

However, λ only distinguishes sample hardness at the data level and is calculated offline, which may misalign β adjustment with the model’s actual responsiveness. Inspired by [28], we compute the implicit reward gap to capture the model’s current preference between positive and negative samples and guide the update of β .

The reward gap is defined as:

$$\mathcal{R}_i = \left[\beta \log \frac{\pi_\theta(y_{w,i} | x_i, \mathcal{I}_i)}{\pi_{\text{ref}}(y_{w,i} | x_i, \mathcal{I}_i)} - \beta \log \frac{\pi_\theta(y_{l,i} | x_i, \mathcal{I}_i)}{\pi_{\text{ref}}(y_{l,i} | x_i, \mathcal{I}_i)} \right], \quad (7)$$

where π_θ and π_{ref} represent the policy model and reference model, respectively. \mathcal{R}_i corresponds to the reward gap of λ_i for the i -th sample. Then, $\bar{\mathcal{R}}_i = \mathcal{R}_i / (\frac{1}{N} \sum_{i=1}^N \mathcal{R}_i)$ (N denotes the number of samples) is mean-normalized, and a mask vector $\mathcal{M}_i = [0, 1, \dots, 1, 0]$ filters out the two most extreme samples with the lowest and highest values to suppress outliers.

$$\eta = \sigma \left(\frac{1}{N-2} \sum_{i=1}^N \mathcal{M}_i \bar{\mathcal{R}}_i \right) / \sigma(\bar{\mathcal{R}}). \quad (8)$$

where η is the estimated model responsiveness, and $\bar{\mathcal{R}}$ denotes data’s estimated average reward gap. In other words, λ measures the intrinsic difficulty of the data, while η reflects the model’s learning status. The model responsiveness allows β to account for both sample difficulty and real-time training dynamics, compensating for limitations of similarity-based signals, and helps DPO avoid overfitting on easy samples and underfitting on hard ones, ensuring more stable and efficient optimization.

3.2 Noise-regularized Distribution Optimization

In this section, we aim to mitigate the cross-modal semantic bias in MLLMs through the distribution optimization strategy of DPO. As shown in Figure 2 (a), before training, title embeddings (in language space) and image embeddings (in visual space) remain separated in the semantic space, increasing the risk of modality bias. At this point, the policy and reference models are untrained, and their distributions stay closely aligned. Without intervention, DPO training leads to a “the weak get weaker” trend in Figure 2 (b). The output distributions of DPO show that, under the strong reverse KL constraint [53], policy model π_θ concentrates in high-probability regions of the reference model, further reducing similarity between misaligned title–image pairs.

In such cases, the policy model behaves too similarly to the reference model, limiting its ability to overcome modality bias. To address this, we inject moderate Gaussian noise [4, 48] into the output distributions of the policy model to increase modal flexibility.

$$\tilde{\pi}_\theta(y | x, \mathcal{I}) = \mathbb{E}_{\epsilon \sim \mathcal{N}(0, \mathbf{I})} [\pi_\theta(y | x, \mathcal{I}; \mathbf{z} + \epsilon \odot \mathbf{z})]. \quad (9)$$

where \mathbf{z} denotes the last-layer logits of π_θ before generating the output distributions. Given the large number of base parameters and the use of LoRA fine-tuning [18], we express the weights as $W = W_0 + BA$, where $A \in \mathbb{R}^{r \times d}$ and $B \in \mathbb{R}^{d \times r}$. During forward propagation, the LoRA increment is temporarily perturbed.

$$\begin{aligned} A' &= A + \sigma_n \epsilon_A, \quad \epsilon_A \sim \mathcal{N}(0, \mathbf{I}) \\ B' &= B + \sigma_n \epsilon_B, \quad \epsilon_B \sim \mathcal{N}(0, \mathbf{I}) \end{aligned} \quad (10)$$

and we compute the logits $W' = W_0 + B'A'$. This applies noise regularization to the trainable parts of π_θ and π_{ref} , resulting in naturally smoothed output distributions. As DPO training progresses through iterations, the Gaussian-smoothed distributions are incorporated into the similarity-aware adaptive KL divergence loss. Finally, as shown in Figure 2 (c), training leads to a more convergent semantic space with reduced modality bias. The joint optimization with Gaussian perturbation and adaptive KL regulation gradually aligns title and image embeddings toward a shared semantic center.

3.3 Model Optimization

In a mini-batch, we define $\mathcal{B} = \{(x_i, \mathcal{I}_i, y_{w,i}, y_{l,i})\}_{i=1}^B \sim \mathcal{D}$ to analyze the optimization process during each epoch. We first calculate the data hardness for each sample pair, and then derive $\lambda_{\mathcal{B}} = \{\lambda_1, \lambda_2, \dots, \lambda_B\}$ based on the batch partition B , and obtain the corresponding model responsiveness $\eta_{\mathcal{B}} = \{\eta_1, \eta_2, \dots, \eta_B\}$. Next, we filter out outliers in $\eta_{\mathcal{B}}$ using Eq. (8) to obtain the batch-level model responsiveness $\bar{\eta}_{\mathcal{B}}$. We then compute the final weight for each sample through a dynamic combination method:

$$\beta'_{\mathcal{B}} = \bar{\eta}_{\mathcal{B}} \cdot \lambda_{\mathcal{B}} \cdot \beta_0, \quad (11)$$

where β_0 is the initial value, typically set to 0.1. This combination of HaRS enables the model to perceive data hardness while leveraging model responsiveness to enhance optimization robustness.

Moreover, NoDO adaptively integrates Gaussian noise with implicit KL divergence [34] in DPO to pull high-similarity pairs closer and push hallucinated pairs apart, reducing cross-modal semantic bias. Finally, the revised DPO loss is presented as loss $\mathcal{L}_{\text{HaNo}}$:

$$\begin{aligned} \mathcal{L}_{\text{HaNo}} = -\mathbb{E}_{(\mathcal{I}, x, y_w, y_l)} &[\log \sigma \left(\beta' \log \frac{\tilde{\pi}_\theta(y_w | \mathcal{I}, x)}{\pi_{ref}(y_w | \mathcal{I}, x)} \right) \\ &- \beta' \log \frac{\tilde{\pi}_\theta(y_l | \mathcal{I}, x)}{\pi_{ref}(y_l | \mathcal{I}, x)}], \end{aligned} \quad (12)$$

where $\tilde{\pi}_\theta$ and β' represent the perturbed policy model and its corresponding adaptive dynamic DPO weight, respectively. The two modules collaborate to help the model focus on hard examples while preserving stable cross-modal alignment, addressing our proposed challenges in MLLM-based sequential recommendation.

4 Experiments

In this section, we conduct extensive experiments and answer the following research questions:

- **RQ1:** How does HaNoRec compare to the current state-of-the-art (SOTA) framework in terms of performance?
- **RQ2:** Are the key components in our HaNoRec delivering the expected performance gains?
- **RQ3:** What are the reasons for model's superior performance?
- **RQ4:** How do different hyperparameters affect HaNoRec?

4.1 Experiment Setup

4.1.1 Datasets. We evaluate our model on three multimodal datasets: Microlens [30], Netflix [50], and MovieLens-1M¹. Appendix B provides details on data collection.

4.1.2 Baselines. Our HaNoRec employs the Qwen as the backbone to serve as a sequential recommender. Therefore, we divide the baselines into traditional, LLM-based, and MLLM-based recommendation methods.

Traditional RS. GRU4Rec [16] uses GRU [8] to construct a session-level sequential model for next-click prediction. SASRec [21] models the user's historical behavior sequence using a self-attention mechanism. LightGCN [14] removes the feature transformation and nonlinear activations of GCN for light recommendation. LATTICE [60] constructs a latent item-item graph to enhance multimodal recommendation performance. CL4SRec [52] is the first to introduce contrastive learning into SR. MoRec [56] explores whether pure modality information can replace traditional item ID representations. RecDCL [58] applies both batch-wise and feature-wise contrastive learning to collaborative filtering.

LLM-based RS. TallRec [6] proposes supervised fine-tuning of large language models to adapt them for recommendation tasks. LLaRA [26] designs a recommendation assistant that combines collaborative filtering signals with language models. SPRec [12] leverages a self-play mechanism in LLMs to de-bias and guide the model toward more balanced outputs.

MLLM-based RS. MSRbench [67] evaluates the capability of vision-language multimodal large models in SR. MLLM-MSR [54] fine-tunes multimodal LLMs to specialize them for SR tasks.

4.1.3 Metrics. We evaluate model performance using AUC, HR@3, and NDCG@3. AUC is used to assess the binary decision of whether the user will like a target item. HR@3 and NDCG@3 are employed to measure the model's Top-K ranking ability. AUC does not require a candidate set, while HR and NDCG use the prediction target along with 9 randomly sampled negative items to form a candidate set of 10. The size of the candidate item set is standardized across all methods for fair comparison.

4.1.4 Implementations. To ensure fairness, both our experiments and baselines are conducted on a Linux server equipped with 8 A5880 GPUs. We use Qwen-2.5-3B-Instruct² and Qwen-2.5-VL-3B-Instruct³ as the base models for the LLM-based and MLLM-based backbones, respectively. LLM-based models are trained for 10 epochs, and MLLM-based models for 5. During the training of HaNoRec, we consistently set the LoRA rank to 8, the learning rate to 1e-4, and the gradient accumulation steps to 8. Following the setup of [26], all datasets are split into training, validation, and test

¹<https://grouplens.org/datasets/movielens/>

²<https://huggingface.co/Qwen/Qwen2.5-3B-Instruct>

³<https://huggingface.co/Qwen/Qwen2.5-VL-3B-Instruct>

Table 1: Recommendation performance comparisons on different datasets. The superscript * indicates the Imprvement is statistically significant where the p-value is less than 0.05. Bold indicates the best results, and underline is the second-best.

	Model	Year	Microlens			Netflix			Movielens-1M		
			AUC	HR@3	NG@3	AUC	HR@3	NG@3	AUC	HR@3	NG@3
Traditional	GRU4Rec [16]	ICLR'16	0.6980	0.6052	0.4683	0.6347	0.5521	0.4779	0.6942	0.6374	0.4656
	SASRec [21]	ICDM'18	0.7128	0.5970	0.4588	0.6470	0.5781	0.4986	0.7131	0.6467	0.4780
	LightGCN [14]	SIGIR'20	0.7035	0.6070	0.4669	0.6465	0.5625	0.4822	0.7025	0.6308	0.4710
	LATTICE [60]	MM'21	0.7247	0.6369	0.4875	0.6621	0.6042	0.5126	0.7164	0.6424	0.4672
	CL4SRec [52]	ICDE'22	0.7320	0.6515	0.5102	0.6820	0.6250	0.5230	0.7240	0.6556	0.4804
	MoRec [56]	SIGIR'23	0.7144	0.6294	0.4863	0.6784	0.6406	0.5326	0.6824	0.6159	0.4536
LLM-based	TextRec [6]	Recsys'23	0.7253	0.6480	0.4918	0.6927	0.6788	0.5533	0.7303	0.6606	0.4815
	LLaRA [26]	SIGIR'24	0.7375	0.6504	0.4894	0.7178	0.6892	0.5592	0.7392	0.6705	0.4900
	SPRec [12]	WWW'25	0.7450	0.6682	0.4938	0.7378	0.7042	0.5663	0.7380	0.6856	0.4932
MLLM-based	MSRBench [67]	WWW'25	0.7418	0.6650	0.4942	0.7201	0.7020	0.5654	0.7312	0.6846	0.4913
	MLLM-MSR [54]	AAAI'25	0.7544	0.6776	0.5110	0.7448	0.7135	0.5754	0.7497	0.7123	0.5031
	HaNoRec(Ours)		0.7852*	0.7360*	0.5673*	0.7710*	0.7483*	0.6191*	0.7732*	0.7599*	0.5403*
	Improv. %		4.12%	8.62%	11.02%	3.52%	4.88%	7.59%	3.13%	6.68%	7.39%

sets in an 8:1:1 ratio based on the number of sequences. Due to the limited sequence length of the datasets, all models use only the most recent 6 interactions, with the last one serving as the prediction target. Furthermore, we use the same data for training and testing all traditional baseline methods.

4.2 Performance Comparisons(RQ1)

Table 1 shows the performance improvements of HaNoRec on three public datasets. We further discuss interesting observations in the results and provide possible explanations. All experimental results are averaged over five runs.

4.2.1 Limitations of Traditional Methods. Sequential and collaborative filtering models rely on abundant interactions, while our data remains highly sparse (even with truncation on Movielens). Although CL4SRec, the strongest among them, uses contrastive learning-based sequence augmentation to ease the loosely defined cold-start issue, it still falls behind the LLM-based method SPRec by 1.8%, 8.2%, and 1.9% in AUC across the three datasets, highlighting the performance bottleneck in sparse scenarios.

4.2.2 Limitations of LLM-based Methods. Existing LLM-based SR methods typically rely on supervised fine-tuning (SFT), which focuses on historical behaviors but overlooks fine-grained shifts in user preferences. SFT tends to overexpose popular items, reducing diversity and introducing bias. In addition, text-only LLMs cannot leverage multimodal information like images, making it hard to address modality bias from ambiguous titles [59]. For example, as shown in the green part of Table 1, all three LLM methods lag behind the MLLM-based MLLM-MSR by over 8% in HR and NDCG on the sparsest dataset, Microlens, reinforcing our motivation.

4.2.3 Superiority of HaNoRec. As shown in Table 1, our model outperforms all baselines across all metrics, with gains of 11.02% on Microlens, 7.59% on Netflix, and 7.39% on Movielens, demonstrating its effectiveness in capturing evolving user preferences. Notably, the NG@3 metric improves significantly, indicating more diverse

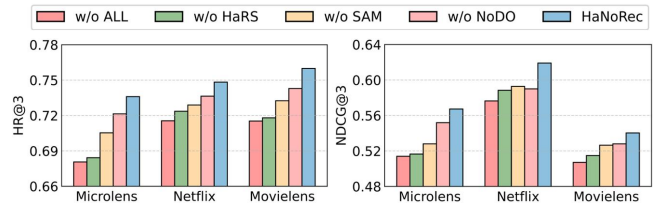


Figure 3: Ablation studies of model variants on the all datasets w.r.t. HR@3 and NDCG@3.

and relevant recommendations while maintaining ranking quality and reducing popularity bias.

Overall, under experimental setting [12], performance shows a clear decline from MLLM-based to LLM-based to traditional methods. Traditional models rely on historical clicks and struggle with sparse interactions. LLM-based methods offer strong language reasoning but overlook visual signals, such as cover images that often serve as the first cue in real scenarios. In contrast, MLLMs capture fine-grained semantics like genre and emotion from item posters, leading to slower performance degradation. Growing evidence [23, 43] also shows that MLLMs increasingly understand images well, supporting the promise of this research direction.

4.3 Ablation Study (RQ2)

4.3.1 Impact of key components. In this section, we assess the impact of key components in HaNoRec and provide potential explanations. The following model variants are evaluated:

- HaNoRec w/o ALL: Removes all proposed components, only “SFT + DPO” training paradigm is conducted;
- HaNoRec w/o HaRS: Removes the Hardness-aware reweighting strategy (HaRS) module in Sec. 3.1;
- HaNoRec w/o SAM: Removes the Top-K sampling strategy within the HaRS component;
- HaNoRec w/o NoDO: Removes noise-regularized distribution optimization (NoDO) module in Sec. 3.2.

Table 2: Ablation studies of different MLLMs on three datasets w.r.t. AUC, HR@3 and NDCG@3.

Variants	Microlens			Netflix			Movielens		
	AUC	H@3	N@3	AUC	H@3	N@3	AUC	H@3	N@3
Qwen2-VL-2B [46]	0.7780	0.7338	0.5664	0.7724	0.7417	0.6130	0.7704	0.7486	0.5410
Qwen2.5-VL-3B [3]	0.7852	0.7360	0.5673	0.7710	0.7483	0.6191	0.7732	0.7599	0.5403
Qwen2.5-VL-7B [3]	0.7890	0.7421	0.5756	0.7816	0.7527	0.6238	0.7785	0.7623	0.5408
LLaVA-NeXT-7B [23]	0.7957	0.7446	0.5805	0.7892	0.7514	0.6198	0.7831	0.7635	0.5422

Figure 3 presents the experimental results on the all datasets, leading to the following insights:

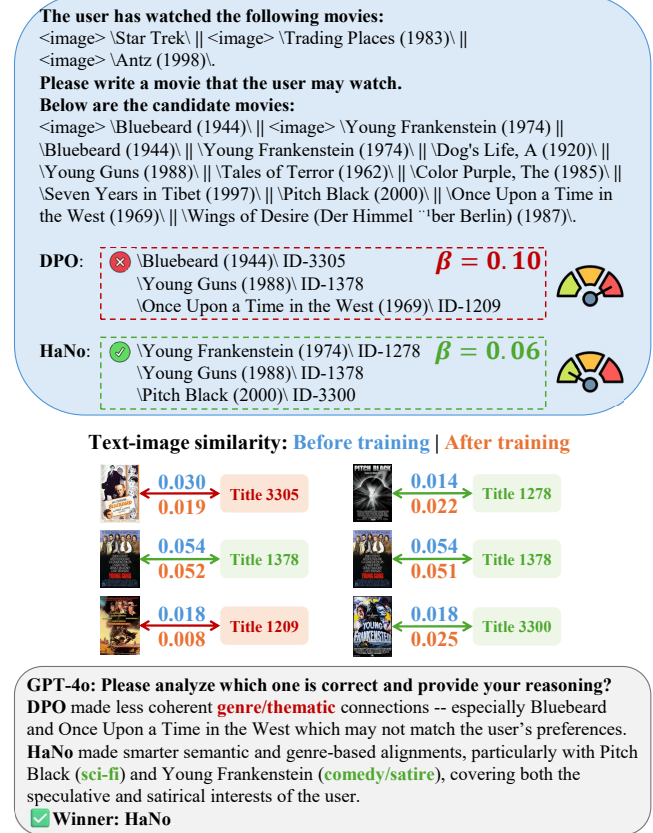
Experimental results show that HaRS has the greatest impact on recommendation performance; without it, results often resemble those of the base model. This indicates that dynamically scaling the DPO weight effectively captures sample hardness and guides the model to focus on “hard-to-distinguish” samples, while assigning lower weights to “easy-to-distinguish” ones to avoid overfitting on simple patterns [28]. This is attributed to the fact that multiple positives capture diverse preference signals, while stratified negatives form a difficulty gradient that enhances ranking precision.

Subsequently, we further analyze the NoDO module. While its performance gain is modest, it addresses the modality bias in MLLM-based SR through a simple and effective Gaussian noise perturbation method. In a nutshell, all components improve accuracy when built upon “SFT + DPO” paradigm, highlighting the importance of preference optimization and distribution optimization in fully leveraging MLLMs’ potential for sequential recommendation.

4.3.2 Impact of different MLLMs. To evaluate the impact of different MLLMs as backbones, we run experiments with various Qwen-VL series and sizes, along with the widely used LLaVA-NeXT. As shown in Table 2, 2B models perform worst, while 7B versions of Qwen and LLaVA generally perform best, indicating that MLLM-based recommendation follows the large model scaling law [22]. However, performance gains do not scale proportionally with time cost. The performance gap between LLaVA and Qwen may result from differences in their visual encoders and cross-modal alignment strategies. Overall, the generalization experiments confirm that our approach is model-agnostic and transferable, supporting its application to broader multimodal recommendation scenarios.

4.4 Case Study (RQ3)

This section presents a case study of user 4126 from the Movielens dataset. As shown in the blue region of Figure 4, given the interaction history and candidate set as a prompt, DPO produces an incorrect recommendation, while HaRS identifies the correct one. HaNoRec computes the sample’s hardness and model responsiveness, assigning a weight of 0.06, indicating it is hard to distinguish. HaRS relaxes the KL constraint and retrieves **Young Frankenstein**, which matches the user’s preference style. In contrast, DPO with fixed weighting recommends only popular but irrelevant items. Next, we compute the title–image similarity scores before and after training for the six movies retrieved by DPO and HaRS. Except for the top-scoring movie 1378, which slightly drops, DPO shows a significant decline in similarity for other movies, while HaRS improves the scores of its retrieved items. This supports **Challenge**

**Figure 4: Case study on Movielens for user 4126.**

2, showing that NoDO effectively mitigates title–image mismatch caused by MLLM modality bias.

Finally, we conduct a blind test using GPT-4o [19], asking it to judge which recommendation list better matches the user based solely on historical interactions, without access to ground truth. As shown in the gray region of figure, GPT-4o finds that HaRS’s recommendations better align with the user’s interests in genre and semantics (sci-fi and dark comedy), while DPO’s list lacks thematic coherence, leading to the verdict: **Winner: HaNo**.

4.5 Hyperparameter Sensitivity (RQ4)

In this study, we keep HaNoRec parameters fixed and individually analyze the Top-K similar item group in HaRS, the Gaussian noise strength in NoDO, and the initial DPO weight, corresponding to K in Eq. (5), σ_n in Eq. (10) and β_0 in Eq. (11).

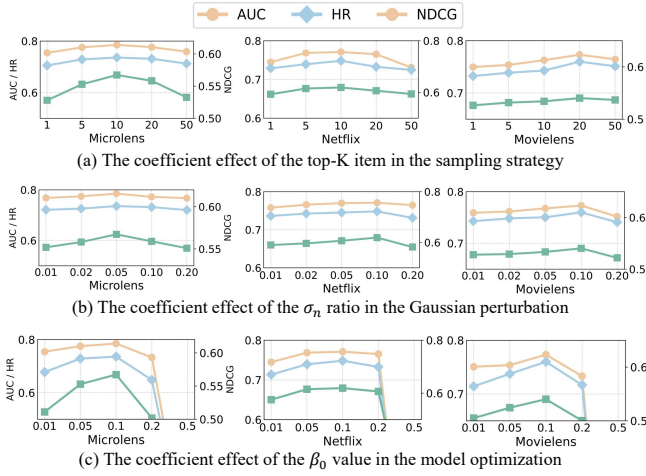


Figure 5: Performance comparison w.r.t. different hyperparameters. The y-axes on the left belong to the metrics AUC and HR and the right belong to NDCG.

- As shown in Figure 5 (a), HaRS performs best when Top-K is set to 10 or 20. Too small (K=1) or too large (K=50) values lead to failure. With only one sample, it cannot capture multi-dimensional preferences; with too many weak or incorrect samples, the boundary between positive and negative clusters becomes unclear. In both cases, overly simple or noisy samples distort the hardness curve, making it hard for HaRS to focus on truly difficult instances and weakening optimization.
- As observed from the figure, σ_n , the strength of Gaussian noise, has limited impact on performance. While 0.05 works best for Microlens, 0.1 is optimal for other datasets. A larger weight introduces stronger LoRA [18] perturbations, smoothing the distribution more—beneficial for datasets like Netflix with low-variance visual features. In contrast, a smaller weight provides milder perturbation and more stable distributions, which suits high-variance datasets like Microlens.
- Finally, in part (c), we evaluate how different β values affect the model. As the base coefficient increases, the model enlarges the positive–negative probability gap more rapidly, improving recommendation accuracy. When $\beta = 0.5$, performance drops significantly, as the DPO weight becomes too large, disrupting the fixed response pattern established during SFT.

5 Related Work

5.1 LLMs and MLLMs for Recommendation

Large language models (LLMs) have gained significant attention in recommender systems for their advanced language understanding and reasoning abilities. Research in this area primarily follows three paradigms: LLMs as recommenders, enhancers, and encoders. LLMs as recommenders [26, 57]: These methods use user interaction histories as prompts to guide LLMs in selecting recommendation targets from a candidate set. TallRec [6] fine-tunes Llama on constructed recommendation datasets, enhancing LLM decision-making in recommendations. RosePO [25] employs smoothing personalized preference optimization to fine-tune LLMs, improving

performance while ensuring the recommender remains “helpful and harmless”. LLMs as enhancers [32, 48, 62]: RLMRec [37] introduces a framework leveraging LLM-driven representation learning, with contrastive and generative alignment methods to improve recommendations. AlphaRec [41] replaces ID-based embeddings with language embeddings and combines GCN and CL for a simple yet effective recommendation approach. LLMs as encoders [13, 17]: EasyRec [35] leverages collaborative information and textual data from users and items to retrain language models for recommendation, achieving impressive performance in zero-shot scenarios.

To extend LLM-based recommenders to multimodal scenarios, researchers explore multimodal large language models (MLLMs) that integrate visual and textual information to better capture user preferences. Rec-GPT4V [27] introduces a visual summarization reasoning mechanism to improve user modeling and reduce dynamic image redundancy. MSR Bench [67] conducts a systematic evaluation of different MLLM integration strategies and highlights computational inefficiency as a key challenge. MLLM-MSR [54] designs a two-stage user modeling framework that combines image summarization with sequence modeling to fine-tune MLLMs.

5.2 Preference Alignment in MLLMs

Recent advances in large-scale human preference data [20] and reinforcement learning (RL) techniques [31] have made preference alignment a key driver in the development of LLMs and MLLMs. In MLLMs, preference alignment research primarily focuses on two aspects: (I) constructing high-quality preference datasets [24, 55] and (II) designing effective alignment optimization strategies [29, 34]. Within the first direction, RLAIF-V [55] emphasizes a self-feedback alignment mechanism that spans both training and inference stages, while VLFeedback [24] focuses on large-scale automatically generated offline preference data. For alignment optimization strategies, the dominant methods are built upon the RL framework, adopting proximal policy optimization (PPO [40]) or the simplified direct preference optimization (DPO [34]) variant. For example, RLHF-RLAIF [43] improves reward design by incorporating vision-language factual enhancement and hallucination penalty mechanisms to enhance multimodal alignment. Povid [68] generates AI preference data by injecting hallucinations and applying image perturbations, enabling feedback construction without human involvement. However, PPO-based methods face issues such as training complexity and poor stability [45]. Building on this, HA-DPO [65] enhances hallucination robustness by constructing consistent positive and negative sample pairs, while OPA-DPO [53] alleviates this phenomenon by addressing the KL divergence in alignment strategy training. Subsequently, DAMO [28] dynamically adjusts the optimization strategy from both the data and model perspectives, revisiting the distinguishability of negative samples.

6 Conclusion

This paper leveraged the capability of Multimodal Large Language Models (MLLMs) in understanding and generating multimodal information to improve sequential recommendation accuracy. We proposed a user preference learning framework, HaNoRec, which dynamically scaled the weight of the preference model based on hardness-aware reweighting strategy to focus on difficult samples

and accurately capture the evolution of user preferences, while also incorporating model responsiveness to improve optimization robustness. Additionally, we divedes a noise-regularized distribution optimization objective to mitigate cross-modal bias via Gaussian noise perturbation and adaptive KL regularization. Experiments on three public datasets demonstrated the superiority of HaNoRec.

References

- [1] Josh Achiam, Steven Adler, Sandhini Agarwal, Lama Ahmad, Ilge Akkaya, Florencia Leoni Aleman, Diogo Almeida, Janko Altenschmidt, Sam Altman, Shyamal Anadkat, et al. 2023. Gpt-4 Technical Report. *arXiv preprint arXiv:2303.08774* (2023).
- [2] Alexander A Alemi, Ian Fischer, Joshua V Dillon, and Kevin Murphy. 2017. Deep Variational Information Bottleneck. In *ICLR*.
- [3] Shuai Bai, Keqin Chen, Xuejing Liu, Jialin Wang, Wenbin Ge, Sibo Song, Kai Dang, Peng Wang, Shijie Wang, Jun Tang, Humen Zhong, Yuanzhi Zhu, Mingkun Yang, Zhaohai Li, Jianqiang Wan, Pengfei Wang, Wei Ding, Zheren Fu, Yiheng Xu, Jiabo Ye, Xi Zhang, Tianbao Xie, Zesen Cheng, Hang Zhang, Zhibo Yang, Haiyang Xu, and Junyang Lin. 2025. Qwen2.5-VL Technical Report. *arXiv preprint arXiv:2502.13923* (2025).
- [4] Zechen Bai, Pichao Wang, Tianjun Xiao, Tong He, Zongbo Han, Zheng Zhang, and Mike Zheng Shou. 2024. Hallucination of Multimodal Large Language Models: A Survey. *arXiv preprint arXiv:2404.18930* (2024).
- [5] Keqin Bao, Jizhi Zhang, Wenjie Wang, Yang Zhang, Zhengyi Yang, Yanchen Luo, Chong Chen, Fuli Feng, and Qi Tian. 2025. A Bi-Step Grounding Paradigm for Large Language Models in Recommendation Systems. *ACM Transactions on Recommender Systems (TORS)* 3, 4 (2025), 1–27.
- [6] Keqin Bao, Jizhi Zhang, Yang Zhang, Wenjie Wang, Fuli Feng, and Xiangnan He. 2023. TallRec: An Effective and Efficient Tuning Framework to Align Large Language Model with Recommendation. In *RecSys*. 1007–1014.
- [7] Jiawei Chen, Hongyu Lin, Xianpei Han, and Le Sun. 2024. Benchmarking Large Language Models in Retrieval-Augmented Generation. In *AAAI*, Vol. 38. 17754–17762.
- [8] Junyoung Chung, Caglar Gulcehre, KyungHyun Cho, and Yoshua Bengio. 2014. Empirical Evaluation of Gated Recurrent Neural Networks on Sequence Modeling. *arXiv preprint arXiv:1412.3555* (2014).
- [9] Sunhao Dai, Chen Xu, Shicheng Xu, Liang Pang, Zhenhua Dong, and Jun Xu. 2024. Bias and Unfairness in Information Retrieval Systems: New Challenges in the LLM Era. In *KDD*. 6437–6447.
- [10] Jacob Devlin, Ming-Wei Chang, Kenton Lee, and Kristina Toutanova. 2019. Bert: Pre-training of Deep Bidirectional Transformers for Language Understanding. In *NAACL*. 4171–4186.
- [11] Abhimanyu Dubey, Abhinav Jauhri, Abhinav Pandey, Abhishek Kadian, Ahmad Al-Dahle, Aiesha Letman, Akhil Mathur, Alan Schelten, Amy Yang, Angela Fan, et al. 2024. The Llama 3 Hurd of Models. *arXiv preprint arXiv:2407.21783* (2024).
- [12] Chongming Gao, Ruijun Chen, Shuai Yuan, Kexin Huang, Yuqiang Yu, and Xiangnan He. 2025. SPRec: Self-Play to Debias LLM-based Recommendation. In *WWW*. 5075–5084.
- [13] Yunfan Gao, Tao Sheng, Youlin Xiang, Yun Xiong, Haofen Wang, and Jiawei Zhang. 2023. Chat-Rec: Towards Interactive and Explainable LLMs-augmented Recommender System. *arXiv preprint arXiv:2303.14524* (2023).
- [14] Xiangnan He, Kuan Deng, Xiang Wang, Yan Li, Yongdong Zhang, and Meng Wang. 2020. Lightgen: Simplifying and Powering Graph Convolution Network for Recommendation. In *SIGIR*. 639–648.
- [15] Xiangnan He, Lizi Liao, Hanwang Zhang, Liqiang Nie, Xia Hu, and Tat-Seng Chua. 2017. Neural Collaborative Filtering. In *WWW*. 173–182.
- [16] Balázs Hidasi, Alexandros Karatzoglou, Linas Baltrunas, and Domonkos Tikk. 2016. Session-based Recommendations with Recurrent Neural Networks. In *ICLR*.
- [17] Yupeng Hou, Jiacheng Li, Zhanhui He, An Yan, Xiusi Chen, and Julian McAuley. 2024. Bridging language and items for retrieval and recommendation. *arXiv preprint arXiv:2403.03952* (2024).
- [18] Edward J Hu, Yelong Shen, Phillip Wallis, Zeyuan Allen-Zhu, Yuanzhi Li, Shean Wang, Lu Wang, Weizhu Chen, et al. 2022. Lora: Low-rank Adaptation of Large Language Models. In *ICLR*.
- [19] Aaron Hurst, Adam Lerer, Adam P Goucher, Adam Perelman, Aditya Ramesh, Aidan Clark, AJ Ostrom, Akila Welihinda, Alan Hayes, Alec Radford, et al. 2024. GPT-4o System Card. *arXiv preprint arXiv:2410.21276* (2024).
- [20] Jiaming Ji, Mickel Liu, Josef Dai, Xuehai Pan, Chi Zhang, Ce Bian, Boyuan Chen, Ruiyang Sun, Yizhou Wang, and Yaodong Yang. 2023. Beavertails: Towards Improved Safety Alignment of LLM via a Human-Preference Dataset. In *NeurIPS*, Vol. 36. 24678–24704.
- [21] Wang-Cheng Kang and Julian McAuley. 2018. Self-attentive Sequential Recommendation. In *ICDM*. 197–206.
- [22] Jared Kaplan, Sam McCandlish, Tom Henighan, Tom B Brown, Benjamin Chess, Rewon Child, Scott Gray, Alec Radford, Jeffrey Wu, and Dario Amodei. 2020. Scaling Laws for Neural Language Models. *arXiv preprint arXiv:2001.08361* (2020).
- [23] Feng Li, Renrui Zhang, Hao Zhang, Yuanhan Zhang, Bo Li, Wei Li, Zejun Ma, and Chunyuan Li. 2024. LLaVA-NeXT-Interleave: Tackling Multi-image, Video, and 3D in Large Multimodal Models. *arXiv preprint arXiv:2407.07895* (2024).
- [24] Lei Li, Zhihui Xie, Mukai Li, Shunian Chen, Peiyi Wang, Liang Chen, Yazheng Yang, Benyou Wang, Lingpeng Kong, and Qi Liu. 2024. VLFeedback: A Large-Scale AI Feedback Dataset for Large Vision-Language Models Alignment. *arXiv preprint arXiv:2410.09421* (2024).
- [25] Jiayi Liao, Xiangnan He, Ruobing Xie, Jiancan Wu, Yancheng Yuan, Xingwu Sun, Zhanhui Kang, and Xiang Wang. 2024. RosePO: Aligning LLM-based Recommenders with Human Values. *arXiv preprint arXiv:2410.12519* (2024).
- [26] Jiayi Liao, Sihang Li, Zhengyi Yang, Jiancan Wu, Yancheng Yuan, Xiang Wang, and Xiangnan He. 2024. Llara: Large Language-Recommendation Assistant. In *SIGIR*. 1785–1795.
- [27] Yiqing Liu, Yu Wang, Lichao Sun, and Philip S Yu. 2024. Rec-GPT4V: Multimodal Recommendation with Large Vision-Language Models. *arXiv preprint arXiv:2402.08670* (2024).
- [28] Jinda Lu, Junkang Wu, Jinghan Li, Xiaojun Jia, Shuo Wang, YiFan Zhang, Junfeng Fang, Xiang Wang, and Xiangnan He. 2025. DAMO: Data-and Model-aware Alignment of Multi-modal LLMs. In *ICML*.
- [29] Yu Meng, Mengzhou Xia, and Dangi Chen. 2024. SimPO: Simple Preference Optimization with a Reference-Free Reward. In *NeurIPS*, Vol. 37. 124198–124235.
- [30] Yongxin Ni, Yu Cheng, Xiangyan Liu, Junchen Fu, Youhua Li, Xiangnan He, Yongfeng Zhang, and Fajie Yuan. 2023. A Content-driven Micro-video Recommendation Dataset at Scale. *arXiv preprint arXiv:2309.15379* (2023).
- [31] Long Ouyang, Jeffrey Wu, Xu Jiang, Diogo Almeida, Carroll Wainwright, Pamela Mishkin, Chong Zhang, Sandhini Agarwal, Katarina Slama, Alex Ray, John Schulman, Jacob Hilton, Fraser Kelton, Luke Miller, Maddie Simens, Amanda Askell, Peter Welinder, Paul F Christiano, Jan Leike, and Ryan Lowe. 2022. Training Language Models to Follow Instructions with Human Feedback. In *NeurIPS*, Vol. 35. 27730–27744.
- [32] Yingtao Peng, Chen Gao, Yu Zhang, Tangpeng Dan, Xiaoyi Du, Hengliang Luo, Yong Li, and Xiaofeng Meng. 2025. Denoising alignment with large language model for recommendation. *ACM Transactions on Information Systems (TOIS)* 43, 2 (2025), 1–35.
- [33] Alec Radford, Jong Wook Kim, Chris Hallacy, Aditya Ramesh, Gabriel Goh, Sandhini Agarwal, Girish Sastry, Amanda Askell, Pamela Mishkin, Jack Clark, et al. 2021. Learning Transferable Visual Models From Natural Language Supervision. In *ICML*. 8748–8763.
- [34] Rafael Radford, Archit Sharma, Eric Mitchell, Christopher D Manning, Stefano Ermon, and Chelsea Finn. 2023. Direct Preference Optimization: Your Language Model is Secretly a Reward Model. In *NeurIPS*, Vol. 36. 53728–53741.
- [35] Xubin Ren and Chao Huang. 2024. EasyRec: Simple yet Effective Language Models for Recommendation. *arXiv preprint arXiv:2408.08821* (2024).
- [36] Xubin Ren, Jiabin Tang, Dawei Yin, Nitesh Chawla, and Chao Huang. 2024. A Survey of Large Language Models for Graphs. In *KDD*. 6616–6626.
- [37] Xubin Ren, Wei Wei, Lianghao Xia, Lixin Su, Suqi Cheng, Junfeng Wang, Dawei Yin, and Chao Huang. 2024. Representation Learning with Large Language Models for Recommendation. In *WWW*. 3464–3475.
- [38] Francesco Ricci, Lior Rokach, and Bracha Shapira. 2010. Introduction to Recommender Systems Handbook. In *Recommender Systems Handbook*. Springer, 1–35.
- [39] Lei Sang, Yu Wang, Yi Zhang, Yiwen Zhang, and Xindong Wu. 2025. Intent-guided Heterogeneous Graph Contrastive Learning for Recommendation. *IEEE Transactions on Knowledge and Data Engineering (TKDE)* 37, 4 (2025), 1915–1929.
- [40] John Schulman, Filip Wolski, Prafulla Dhariwal, Alec Radford, and Oleg Klimov. 2017. Proximal Policy Optimization Algorithms. *arXiv preprint arXiv:1707.06347* (2017).
- [41] Lehang Sheng, An Zhang, Yi Zhang, Yuxin Chen, Xiang Wang, and Tat-Seng Chua. 2025. Language Representations Can be What Recommenders Need: Findings and Potentials. In *ICLR*.
- [42] Fei Sun, Jun Liu, Jian Wu, Changhua Pei, Xiao Lin, Wenwu Ou, and Peng Jiang. 2019. BERT4Rec: Sequential Recommendation with Bidirectional Encoder Representations from Transformer. In *CIKM*. 1441–1450.
- [43] Zhiqing Sun, Sheng Shen, Shengciao Cao, Haotian Liu, Chunyuan Li, Yikang Shen, Chuang Gan, Liang-Yan Gui, Yu-Xiong Wang, Yiming Yang, et al. 2024. Aligning Large Multimodal Models with Factually Augmented RLHF. In *ACL*.
- [44] Ashish Vaswani, Noam Shazeer, Niki Parmar, Jakob Uszkoreit, Llion Jones, Aidan N Gomez, Łukasz Kaiser, and Illia Polosukhin. 2017. Attention is All you Need. In *NeurIPS*, Vol. 30.
- [45] Fei Wang, Wenzuan Zhou, James Y Huang, Nan Xu, Sheng Zhang, Hoifung Poon, and Muhan Chen. 2024. mDPO: Conditional Preference Optimization for Multimodal Large Language Models. In *EMNLP*. 8078–8088.
- [46] Peng Wang, Shuai Bai, Sinan Tan, Shijie Wang, Zhihao Fan, Jinze Bai, Keqin Chen, Xuejing Liu, Jialin Wang, Wenbin Ge, et al. 2024. Qwen2-VL: Enhancing Vision-Language Model's Perception of the World at Any Resolution. *arXiv preprint arXiv:2409.12191* (2024).

[47] Shoujin Wang, Liang Hu, Yan Wang, Longbing Cao, Quan Z Sheng, and Mehmet Orgun. 2019. Sequential Recommender Systems: Challenges, Progress and Prospects. In *IJCAI*. 6332–6338.

[48] Yu Wang, Lei Sang, Yi Zhang, and Yiwen Zhang. 2025. Intent Representation Learning with Large Language Model for Recommendation. In *SIGIR*. 1870–1879.

[49] Jason Wei, Xuezhi Wang, Dale Schuurmans, Maarten Bosma, Fei Xia, Ed Chi, Quoc V Le, Denny Zhou, et al. 2022. Chain-of-Thought Prompting Elicits Reasoning in Large Language Models. In *NeurIPS*, Vol. 35. 24824–24837.

[50] Wei Wei, Xubin Ren, Jiaxin Tang, Qinyong Wang, Lixin Su, Suqi Cheng, Junfeng Wang, Dawei Yin, and Chao Huang. 2024. LLMRec: Large Language Models with Graph Augmentation for Recommendation. In *WSDM*. 806–815.

[51] Jiayang Wu, Wensheng Gan, Zefeng Chen, Shicheng Wan, and Philip S Yu. 2023. Multimodal Large Language Models: A Survey. In *BigData*. IEEE. 2247–2256.

[52] Xu Xie, Fei Sun, Zhaoyang Liu, Shiwen Wu, Jinyang Gao, Jiandong Zhang, Bolin Ding, and Bin Cui. 2022. Contrastive Learning for Sequential Recommendation. In *ICDE*. 1259–1273.

[53] Zhihe Yang, Xufang Luo, Dongqi Han, Yunjian Xu, and Dongsheng Li. 2025. Mitigating Hallucinations in Large Vision-Language Models via DPO: On-Policy Data Hold the Key. In *CVPR*. 10610–10620.

[54] Yuyang Ye, Zhi Zheng, Yishan Shen, Tianshu Wang, Hengruo Zhang, Peijun Zhu, Runlong Yu, Kai Zhang, and Hui Xiong. 2025. Harnessing Multimodal Large Language Models for Multimodal Sequential Recommendation. In *AAAI*, Vol. 39. 13069–13077.

[55] Tianyu Yu, Yuan Yao, Haoye Zhang, Taiwen He, Yifeng Han, Ganqu Cui, Jinyi Hu, Zhiyuan Liu, Hai-Tao Zheng, Maosong Sun, and Tat-Seng Chua. 2024. RLHF-V: Towards Trustworthy MLLMs via Behavior Alignment from Fine-grained Correctional Human Feedback. In *CVPR*. 13807–13816.

[56] Zheng Yuan, Fajie Yuan, Yu Song, Youhua Li, Junchen Fu, Fei Yang, Yunzhu Pan, and Yongxin Ni. 2023. Where to Go Next for Recommender Systems? ID-vs. Modality-based Recommender Models Revisited. In *SIGIR*. 2639–2649.

[57] Zhenrui Yue, Sara Rabhi, Gabriel de Souza Pereira Moreira, Dong Wang, and Even Oldridge. 2023. LlamaRec: Two-Stage Recommendation using Large Language Models for Ranking. In *CIKM Workshop on Personalized Generative AI*.

[58] Dan Zhang, Yangliao Geng, Wenwen Gong, Zhongang Qi, Zhiyu Chen, Xing Tang, Ying Shan, Yuxiao Dong, and Jie Tang. 2024. RecDCL: Dual Contrastive Learning for Recommendation. In *WWW*. 3655–3666.

[59] Jizhi Zhang, Keqin Bao, Yang Zhang, Wenjie Wang, Fuli Feng, and Xiangnan He. 2023. Is ChatGPT Fair for Recommendation? Evaluating Fairness in Large Language Model Recommendation. In *RecSys*. 993–999.

[60] Jinghao Zhang, Yanqiao Zhu, Qiang Liu, Shu Wu, Shuhui Wang, and Liang Wang. 2021. Mining Latent Structures for Multimedia Recommendation. In *MM*. 3872–3880.

[61] Yang Zhang, Fuli Feng, Jizhi Zhang, Keqin Bao, Qifan Wang, and Xiangnan He. 2025. CoLLM: Integrating Collaborative Embeddings Into Large Language Models for Recommendation. *IEEE Transactions on Knowledge and Data Engineering (TKDE)* 37, 5 (2025), 2329–2340.

[62] Yi Zhang, Yiwen Zhang, Yu Wang, Tong Chen, and Hongzhi Yin. 2025. Towards Distribution Matching between Collaborative and Language Spaces for Generative Recommendation. In *SIGIR*. 2006–2016.

[63] Zizhuo Zhang and Bang Wang. 2023. Prompt Learning for News Recommendation. In *SIGIR*. 227–237.

[64] Wayne Xin Zhao, Kun Zhou, Junyi Li, Tianyi Tang, Xiaolei Wang, Yupeng Hou, Yingqian Min, Beichen Zhang, Junjie Zhang, Zican Dong, et al. 2023. A Survey of Large Language Models. *arXiv preprint arXiv:2303.18223* (2023).

[65] Zhiyuan Zhao, Bin Wang, Linke Ouyang, Xiaoyi Dong, Jiaqi Wang, and Conghui He. 2023. Beyond Hallucinations: Enhancing LVLMs through Hallucination-Aware Direct Preference Optimization. *arXiv preprint arXiv:2311.16839* (2023).

[66] Bowen Zheng, Yupeng Hou, Hongyu Lu, Yu Chen, Wayne Xin Zhao, Ming Chen, and Ji-Rong Wen. 2024. Adapting Large Language Models by Integrating Collaborative Semantics for Recommendation. In *ICDE*. 1435–1448.

[67] Peilin Zhou, Chao Liu, Jing Ren, Xinfeng Zhou, Yueqi Xie, Meng Cao, Zhongtao Rao, You-Liang Huang, Dading Chong, Junling Liu, Jae Boum Kim, Shoujin Wang, Raymond Chi-Wing Wong, and Sunghun Kim. 2025. When Large Vision Language Models Meet Multimodal Sequential Recommendation: An Empirical Study. In *WWW*. 275–292.

[68] Yiyang Zhou, Chenhang Cui, Rafael Rafailov, Chelsea Finn, and Huaxiu Yao. 2024. Aligning Modalities in Vision Large Language Models via Preference Fine-tuning. In *ICLR Workshop on Reliable and Responsible Foundation Models*.

Appendix

In the Appendix, we first present the pseudo-code for the complete training of the proposed HaNoRec. Subsequently, we provide a detailed datasets description and prompt construction.

A Algorithm Description

Algorithm 1 presents the complete training procedure of HaNoRec. In each epoch, a mini-batch \mathcal{B} is sampled from the dataset. For both chosen and rejected items, the Top-K similar candidates are selected to form positive and negative sample sets. Based on image–text similarity differences, sample hardness λ is computed. The reward gap \mathcal{R}_i is calculated from the log-ratio of positive and negative samples and normalized into model responsiveness η . These two factors, together with the base value β_0 , are combined to obtain the adaptive weight β'_i . Gaussian noise is injected into the logits of both the policy and reference models to produce the smoothed distribution $\tilde{\pi}_\theta$. The SDPO loss is then computed using β'_i , and LoRA parameters are updated via backpropagation. This process repeats until the model converges with stable cross-modal alignment.

Algorithm 1 Algorithm of HaNoRec

Input: Given a preference dataset $\mathcal{D} = (\mathcal{I}, x, y_w, y_l) \sim \mathcal{D}$, where \mathcal{I} , x , y_w , and y_l represent the image, question (including interaction history and candidate set), chosen response, and rejected response, respectively.

Output: The title of the next predicted item.

1: Initialize the policy model parameters π_θ .

2: **for** epoch in $\{1, 2, \dots, E\}$ **do**

3: **for** $\mathcal{B} = \{(x_i, \mathcal{I}_i, y_{w,i}, y_{l,i})\}_{i=1}^B \sim \mathcal{D}$ **do**

4: $S_w \leftarrow \text{Top-K}\{y_w\}$, $S_l \leftarrow \text{Top-K}\{y_l\}$;

5: obtain $\lambda_{\mathcal{B}}$ with $\{I_w, S_w\}$, $\{I_l, S_l\}$; \triangleright Equ (4) \rightarrow (6)

6: obtain \mathcal{R}_i with $y_{w,i}$ and $y_{l,i}$; \triangleright Equ (7)

7: obtain $\eta_{\mathcal{B}}$ with \mathcal{R}_i ; \triangleright Equ (8)

8: obtain $\tilde{\pi}_\theta$ with noise ϵ_A and ϵ_B ; \triangleright Equ (9) \rightarrow (10)

9: $\lambda_{\mathcal{B}} \leftarrow \{\lambda_1, \lambda_2, \dots, \lambda_B\}$, $\eta_{\mathcal{B}} \leftarrow \{\eta_1, \eta_2, \dots, \eta_B\}$;

10: obtain $\beta'_{\mathcal{B}}$ with $\lambda_{\mathcal{B}}$ and $\eta_{\mathcal{B}}$; \triangleright Equ (11)

11: compute loss w.r.t. $\beta'_{\mathcal{B}}$ and $\tilde{\pi}_\theta$; \triangleright Equ (12)

12: update the gradient and model π_θ .

13: **end for**

14: **end for**

15: **until** The optimization is converged.

B Datasets Details

Our experiments are evaluated on three real-world datasets. A statistical overview of all the datasets is presented in Table 3.

- **Microlens** is a short-video recommendation dataset that includes titles, cover images, and video information. In this work, only titles and images are used for MLLM. The average number of user interactions is 8.79.
- **Netflix** comes from the data collected on Kaggle by LLMRec and is a user-based movie recommendation dataset. Nonetheless, the dataset is highly sparse, with each user interacting with only 5.23 items on average.

Table 3: Statistics of the experimental datasets.

Dataset	#Users	#Items	#Interactions	Density
Microlens	25,411	41,081	223,263	2.1×10^{-4}
Netflix	13,187	17,366	68,933	3.0×10^{-4}
Movielens	6,040	3,952	1,000,209	4.2×10^{-2}

- **Movielens** is a classic movie recommendation dataset, where each movie includes a title, release year, and corresponding poster. It is very dense, with an average sequence length of 165.56.

Due to missing or corrupted images, we re-crawl image links and retrieve visually similar images based on titles to complete the dataset. To ensure reliable sequential signals, we filter out users with interaction sequences shorter than 6, resulting in three datasets with complete multimodal content and sufficient sequence length.

C Prompt Construction

In this section, we introduce the automated construction process of the SFT and DPO datasets used by HaNoRec and baselines.

C.1 SFT Data

As shown in Figure 6, we design two SFT prompt templates for different evaluation metrics. The first is a binary classification template, which presents watched posters, unwatched posters, and a target poster, prompting the model to answer “Yes” or “No” for AUC evaluation. The second is a Top-K ranking template, which shows the user’s historical posters followed by candidate posters and asks the model to return the K most likely movies for HR and NDCG evaluation. A unified output format enables the model to generate probabilities or ranked results consistently, providing a stable foundation for DPO fine-tuning.

C.2 DPO Data

When constructing DPO data, we use the assistant’s response from SFT as the chosen response. For AUC evaluation, the rejected response is the opposite of the chosen “Yes/No” answer. For HR and NDCG, we select K unobserved items from the candidate set as rejected responses. HaNoRec focuses on learning user preferences from difficult samples, while reducing attention to simpler ones.

AUC Prompt

"user"
The user has watched the following movies:
<image> \“Day the Earth Stood Still, The (1951)\”
<image> \“Thing From Another World, The (1951)\”
<image> \“Mad Max (1979)\”
<image> \“Matrix, The (1999)\”
<image> \“Men in Black (1997)\”

The movies the user has not watched, which may be those they do not prefer:
<image> \“His Girl Friday (1940)\”
<image> \“Breaks, The (1999)\”
<image> \“Man and a Woman, A (Un Homme et une Femme) (1966)\”.

Whether the user will like the target movie:
<image> \“Honey, I Blew Up the Kid (1992)\”

"assistant"
"No"

(a) SFT data for metric AUC

HR &NDCG Prompt

"user"
The user has watched the following movies:
<image> \“Day the Earth Stood Still, The (1951)\”
<image> \“Thing From Another World, The (1951)\”
<image> \“Mad Max (1979)\”

Please write a movie that the user may watch. Below are the candidate movies:
<image> \“Designated Mourner, The (1997)\”
<image> \“Escape from New York (1981)\”
<image> \“Men in Black (1997)\”
<image> \“Midsummer Night’s Dream, A (1999)\”
<image> \“Hav Plenty (1997)\”
<image> \“Artemisia (1997)\”
<image> \“Matrix, The (1999)\”
<image> \“Across the Sea of Time (1995)\”
<image> \“Gone in 60 Seconds (2000)\”
<image> \“Tingler, The (1959)\”

"assistant"
"Escape from New York (1981)"
"Men in Black (1997)"
"Matrix, The (1999)"

(b) SFT data for metrics HR and NDCG

Figure 6: The prompt format for SFT paradigm.